Kontinentales Tiefbohrprogramm der Bundesrepublik Deutschland

3-D Induction Log Simulations

Knuth, Neubauer, Strack (Köln)

Model description

For the simulation of induction log soundings in 3-d conductivity structures the assumption of divergence-free electric fields and axial symmetric field behaviour is not valid. In this case the Helmholtz equation must be solved for all three electric field components.

The total electric field has been separated in a primary and secondary field to reach greater numerical accuracy since the transmitter causes not so steep gradients in the secondary field as in the primary field. Thus the following partial differential equation for the secondary field $\vec{E}^S$ must be solved :

$$\nabla \times \nabla \times \vec{E}^S - k^2 \vec{E}^S + \vec{f} = 0 \qquad (1)$$

with

$$k^2 = i\omega\mu(\sigma - i\omega\epsilon) \qquad (2)$$

and

$$\vec{f} := i\omega\mu[(\sigma_m - i\omega\epsilon_m) - (\sigma - i\omega\epsilon)]\vec{E}^P \,. \qquad (3)$$

The numerical solution was obtained by a finite element program package.

2-layer model with different dip angles

We have calculated the electric field components generated by a vertical magnetic dipole, which was located nearby the dipping layer boundary, for dip angles of $0°, 15°, 30°$ und $45°$. The model space was discretisized into 2160 tetrahedrons (Fig 1).

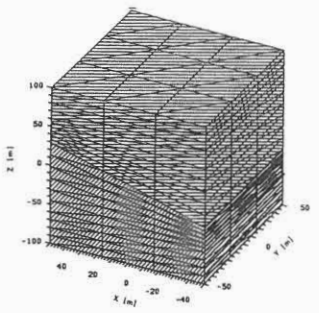

Figure 1 : Finite element grid built-up by 2160 tetrahedrons for a 2-layer model with a dip angle of $30°$.

An significant vertical electric field was observed in the vicinity of the layer boundary. The contourplot in Fig. 2 shows the field distribution on a vertical plane along the strike axis. The dip angle for this model was $\Theta = 45°$. A field structure, antisymmetric both to the layer boundary and to the dipole axis, was recognized.

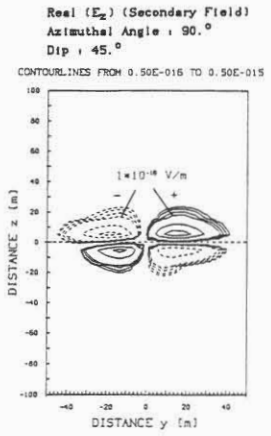

Figure 2 : Contourplot of the E_Z-component on a vertical plane in strike direction ; dip angle $15°$; conductivity contrast $\sigma_2/\sigma_1 = 2$.

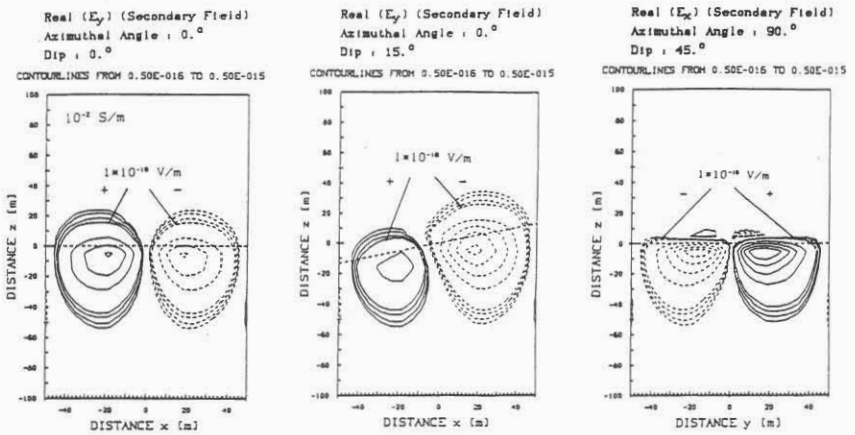

Figure 3 : Contourplot of the E_Y-component on a vertical plane in dip direction for dip angles of $0°$ (left) and $15°$ (middle) and of the E_X-component on a vertical plane in strike direction for a dip angle of $45°$ (right); conductivity contrast $\sigma_2/\sigma_1 = 2$.

The left plot in Fig. 3 shows clearly the exact axial-symmetric field distribution of the E_Y-component at a dip angle of $\Theta = 0°$. At a dip angle of $\Theta = 15°$ (middle plot) the maximum of the positive electric field values (solid lines) has changed its position, whereas the maximum of the negative electric field values (dashed lines) holds its position.

Further, the total value of the maximum amplitude of the negative electric field increases with greater dip angles whereas the total value of the maximum amplitude of the positive electric field shows a even stronger decrease with greater dip angles. These significant dip angle dependency also can be observed for higher conductivity contrasts but with a weaker decrease of the maximum amplitude for positive field values.

These two effects show clearly that the negative E_Y-field values are dominant in the vicinity of the transmitter.

The field distribution of the E_X-component on a vertical plane along the strike axis is shown on the right plot of Fig. 3 for a dip angle of $45°$. In this case the field structure remains its axial symmetry but the field gradient perpendicular to the layer boundary becomes stronger. Conditional on the discontinuity of the E_X-component at the dipping layer boundary a significant declination of the contourlines can be observed in the upper part of the layer transition zone. This effect becomes more important with higher conductivity contrasts.

What consequences are implied by the dipping layers on the receiver signal ?

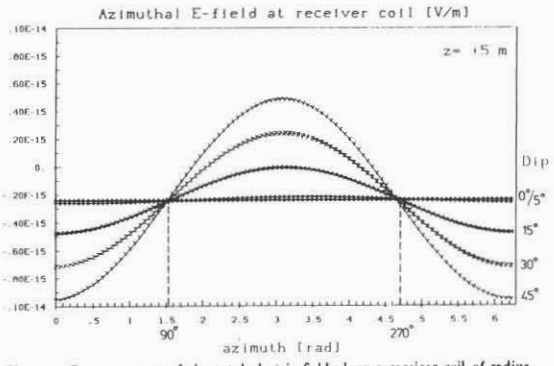

Figure 4: E_Φ-component of the total electric field along a receiver coil of radius $\rho = 0.1\,m$ and dip angles of $0°, 5°, 15°, 30°$ and $45°$; transmitter-receiver distance $L = 1\,m$; conductivity contrast $\sigma_2/\sigma_1 = 2$; coil position $5\,m$ below the intersection axis of the layer boundary.

Therefore we have calculated the azimuthal component of the total electric field for a receiver coil of radius $\rho = 0.1\,m$, which was located in a distance of $L = 1\,m$ above the transmitter. Fig. 4 displays this component for dip angles of $0°, 5°, 15°, 30°$ und $45°$ in dependency of the azimuthal angle. The coil pair was located in the lower layer ($\sigma_2 = 2 \cdot 10^{-2}\,S/m$) $5\,m$ below the conductivity boundary. Already for small dip angles a cosine-like field behaviour was observed. The amplitude of this cosine-like function increases both with greater dip angles and with greater layer conductivities. All curves shown in this figure intersect the non-dipping-layer signal ($\Theta = 0°$) exactly at $\Phi = 90°$ and $\Phi = 270°$. These two azimuthal angles define the intersection axis of the dipping layer.

Conclusions and future developments

It was shown that a dipping layer causes significant changes in the electric field structure, especially for the vertical component near the layer boundary and for the azimuthal component.

An analysis of the azimuthal electric field component shows a strong dip angle dependence of the receiver signal, resulting in a systematic modification of the apparent resistivity. The strong correlation between dip angle and apparent resistivity could be used for the correction of the apparent layer thickness.

In the future apparent resistivities will be calculated for realistic induction tools (e.g. 6FF40). The results are applicable for induction soundings both in the KTB drillhole and in other drill holes with moderate mud conductivity.